Journal of Nuclear Materials 415 (2011) S881–S885

Contents lists available at ScienceDirect

Journal of Nuclear Materials

journal homepage: www.elsevier.com/locate/jnucmat

Integrated models to study the impact of ELMs and disruptions on lithium in the NSTX divertor

Valeryi Sizyuk *,[1], Ahmed Hassanein

School of Nuclear Engineering, Purdue University, West Lafayette, IN 47907, USA

ARTICLE INFO

Article history:
Available online 4 December 2010

ABSTRACT

Lithium as a potential plasma-facing material has many attractive features including a reduction in recycling of hydrogenic species and ability to withstand high heat and neutron fluxes in fusion reactors. Recent analysis of the National Spherical Torus eXperiment (NSTX) device has shown significant and recurring benefits of lithium coatings on plasma-facing components performance. To self-consistently study the performance of lithium divertor during ELMs and disruptions in NSTX, integrated multi-fluid and multi-dimensional models are being developed based on HEIGHTS simulation package that address and combine several areas from the bulk plasma energy released to the magneto-hydrodynamic evolution and production of lithium plasma in the complex magnetic field structure. The simulation showed the importance of the 3D geometrical effects on divertor erosion dynamics. Lithium expansion in divertor and SOL areas may potentially cause bulk plasma contamination during high power ELMs.

1. Introduction

Future fusion reactors with high temperature coolants and extremely high stationary and transient peak power loads may not be realized without the use of liquid metals with new engineering and innovative design approaches [1]. Recent experiments showed that lithium can successfully be used as tokamak plasma-facing components (PFCs) [2]. Similar to boronization [2–4], the lithium-coated wall (lithiation) can significantly enhance plasma performance such as better plasma confinement, purity, and higher density limit. The optical spectral lines of high- and low-*Z* impurities practically disappear from plasma radiation after tokamak lithiation. The hydrogen-recycling coefficient also significantly dropped after tokamak lithiation [2]. Liquid metals could in principle provide heat removal, elimination of erosion concerns via constant renewal of the wall, and possible stabilization of MHD modes by substituting a moving conducting wall for plasma rotation. A crucial issue of tokamaks with lithium coating is lithium contamination of core plasma, particularly during high power transients. Recent studies in the National Spherical Torus eXperiment (NSTX) continue to show significant and recurring benefits of lithium application on PFCs as to the reduction in the recycling of hydrogenic species and the potential for withstanding high heat and neutron fluxes in fusion reactors. The basic concept of the liquid lithium divertor (LLD) design is a toroidally extended lithium-containing tray that will serve as a target for the outer strike point or divertor. The NSTX is a large spherical tokamak with plasma major and minor radii of 0.85 m and up to 0.67 m, respectively [5]. Modeling of divertor operating regimes is of particular importance for heat and particle control prediction in high performance tokamak plasmas, because of the magnetic geometry effects and compactness of the divertor region. In this paper we present our modeling of the NSTX liquid lithium divertor [6] heat load and lithium plasma evolution in the near-divertor area during both Type-I ELM [6,7] and disruptions.

2. Mathematical and physical models

Integrated multi-dimensional, multi-fluid, and multi-processes models were developed for accurate simulation of plasma evolution and interaction with the tokamak wall and divertor components. The SOL plasma was simulated as particles inflow into the divertor area. The initial parameters of the SOL plasma used in our Monte Carlo description were taken from Ref. [8]. The MHD calculations were performed assuming a typical magnetic field initial configuration [9] in the divertor area that was reconstructed in our HEIGHTS package using a set of currents. The detail evolution of the dynamics of plasma in SOL and the resulting kinetic effects are planned for our future model improvement. HEIGHTS integrated models and computer package was upgraded and expanded to full 3D simulation of the interaction of ELM and disrupting

* Corresponding author. Address: Purdue University, 400 Central Drive, West Lafayette, IN 47907, USA.
E-mail addresses: vsizyuk@purdue.edu (V. Sizyuk), hassanein@purdue.edu (A. Hassanein).
[1] Presenting author.

0022-3115/$ - see front matter © 2010 Elsevier B.V. All rights reserved.
doi:10.1016/j.jnucmat.2010.11.080

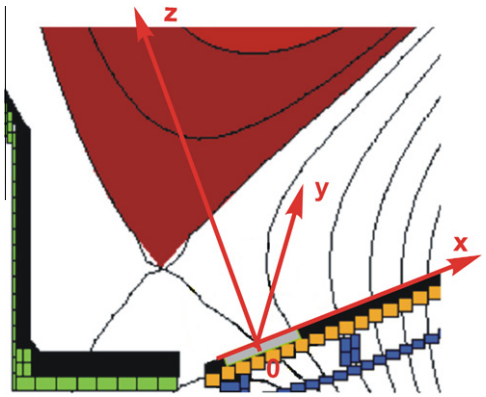

Fig. 1. Schematic of NSTX liquid lithium divertor and orientation of the coordinate system used in the simulation [6].

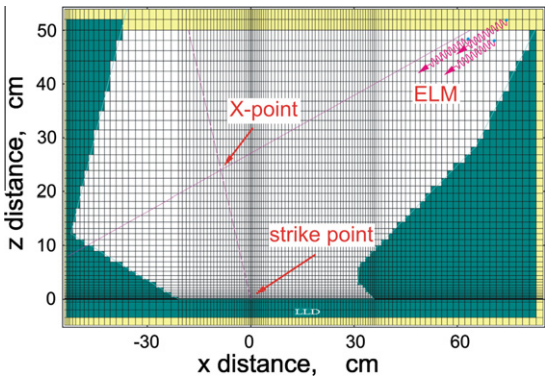

Fig. 2. Computational domain and mesh structure used for NSTX simulation.

plasma in NSTX using lithium divertor. The upgraded HEIGHTS models included four main parts: Monte Carlo block for plasma particles interactions with solid and plasma matter in magnetic field of any configuration; heat conduction and vaporization block for thermal evolution and vaporization of divertor material; magneto-hydrodynamic (MHD) block of near-divertor area plasma evolution; and radiation transport block based on weighted Monte Carlo methods. All blocks were adapted for the case of the outer divertor plate shown in Fig. 1 [6]. Structurally four blocks are combined into the MHD equations system implemented for the three-dimensional case of conservation of mass, momentum, energy, and magnetic field. Because the magnetic field has a complex non-unidirectional structure and a considerable magnitude, the magnetic field energy was separated from the total energy equation and was applied the div(B) correction [10]. Because the NSTX plasma parameters are basically invariable along the divertor surface in the toroidal direction we take zero derivatives of all variables in the y-direction (see Fig. 1 for outer divertor plate). Here we assumed x-axis as poloidal, y-axis as toroidal, and z-axis as radial directions. Fig. 2 schematically illustrates the computational domain of the divertor geometry [6] adapted for calculations. There are many total variation diminishing (TVD) schemes for solving this complicated MHD set of equations, however our choice is second order Lax–Friedrichs (LF) algorithm because it does not use a Riemann solver, thus it can be applied to any system of conservation laws without knowledge of the characteristic waves [11]. The magnetic diffusion corrections were included in the energy and Faraday equations of the MHD system. The magnetic diffusion equations have parabolic type and for its solution we used an implicit method based on sparse matrix formulation. The detailed description of the developed implicit method based on the sparse matrixes for the solution of the magnetic diffusion and heat conduction processes is contained in Ref. [12].

The ELM and disruption plasma impact is simulated using our HEIGHTS Monte Carlo algorithm as the plasma particles flow along the magnetic field of the separatrix [13]. The physical processes that were used for the description of the core plasma particles interaction include: ion–nuclear, ion–electron, electron–nuclear, electron–electron, Bremsstrahlung process, photoabsorption, Compton process, and Auger relaxation. The generation zone of the core plasma particles was located on the right side top domain boundary from the separatrix (see illustration in Fig. 2). The initial energy distributions of plasma particles ensemble and impact durations were taken from the NSTX disruptive plasma parameters [7]. We used the described approach to study the transport of magnetized hot plasma ions and electrons through plasma, lithium vapor, and liquid layers with density, temperature, and magnetic field gradients. Detailed description and benchmarking of HEIGHTS models of plasma particles interaction with matter is published in Refs. [14,15].

We also used our developed Monte Carlo methods for the detail calculations of photon deposition and propagation through the vapor plasma and to nearby components. Detailed description of HEIGHTS 3D Monte Carlo radiation transport model is given in Ref. [16]. The Hartree–Fock–Slater (HFS) and Hartree–Fock (HF) self-consistent field methods are both used to calculate the atomic physics and data needed for lithium. The exchange potential of the HFS method is used in statistical form, while spin–orbit level splitting for non-filled shells is neglected. The HFS equations are solved using iterative methods, yielding wavefunctions, ionization potentials, and energy levels. These values are then used to calculate oscillator strengths of the discrete transitions, photo-ionization cross-sections, line broadening constants, and other atomic data. In calculating the structures of various energy levels and ionization potentials for low-Z elements, we employed the non-relativistic approximation of HFS [17]. The collisional radiative equilibrium (CRE) model was then used to calculate the populations of atomic levels and both ions and electrons concentrations in the lithium plasma produced from further heating of the vaporized lithium. The radiative processes include discrete spontaneous transitions, photorecombination, and dielectronic recombination. Semi-empirical formulas involving the calculated atomic physics data are used to evaluate the cross-sections of these collisional and radiative processes. The processes of radiative excitation and photoionization are neglected in the CRE model. For the optically thick plasma the self-consistent effects due to the non-local radiative flux are taken into account in a simplified form of the escape factor for line transitions and direct photoionization for the continuum spectrum. More detailed description of the plasma properties calculation can be found in Ref. [18].

The initial magnetic field structure of the device is described in the NSTX Team paper [9]. Here, the main component of the magnetic field corresponds to the minus [$0 - Y$] toroidal direction. The field lines in figure [9] represent places with equivalent B_{xz} projection of the magnetic field. The published magnetic field data cannot be used directly for the MHD calculations because of the strong limitation on the divergence value $\nabla \cdot B = 0$. To satisfy this equation, we reconstructed the NSTX magnetic field into the computation domain (Fig. 2) with the assumption of "modeling" current sets [19]. This method, for self-consistency, is concluded in the allocation of "imaginary" current sets that will determine the magnetic field to be equivalent to the experimental values. The calculated magnetic field from such current sets theoretically has zero divergence and is very close to the experimental values. In our model to reconstruct the magnetic field we used four current sets located at distances L from the strike point. For our modeling we assumed initial values

to be used for the complete initialization of the magnetic field in the divertor nearby space: magnetic field $B = 0.5$ T, magnetic field inclined angle at the strike point $\alpha = 5°$, X-point location [−8.6; 23.9] cm in Fig. 2 coordinate system, and distance from X-point to the current line $L \sim 1$ m. The distance L is an adjustable parameter to fit the reconstructed magnetic field to the naturally generated NSTX structure and defines the divertor magnetic system design. The numerical divergence of the reconstructed magnetic field $\nabla \cdot B$ decreases in the computational domain with the increase of the distance L as $\max(\nabla \cdot B|_{L=1\text{m}}) \approx 5 \times 10^{-2}$ Gs/cm and $\max(\nabla \cdot B|_{L=5\text{m}}) \approx 1 \times 10^{-4}$ Gs/cm. For the characteristic scale length of $\delta = 1$ cm, the divergence errors are estimated to be $\left(\frac{\delta \cdot \nabla B}{B}|_{L=1\text{m}}\right) \approx 10^{-5}$ and $\left(\frac{\delta \cdot \nabla B}{B}|_{L=4\text{m}}\right) \approx 10^{-8}$.

3. Simulation results

As noted above and shown in Fig. 2, we trace a large number of the ELM particles trajectories from the SOL up to the divertor. Then we calculate the energy deposition of the ELM plasma particles into the divertor surface to determine lithium vaporization and MHD evolution above the surface. We assumed an exponential distribution of the ELM particles in the SOL space in the x-axis direction [8]. The lithium generated plasma motion changes the magnetic field (i.e., generates current sources) and the currents will also have an effect on the plasma motion. The plasma evolution is different for the ELM and disruption cases and the currents evolution and effects is also different. The initial parameters of the ELM in NSTX device that implemented in our simulation are given as [20]: $Q_{ELM} = 74.0$ kJ total energy of ELM impact; $T_{ELM} = 250$ eV impact plasma temperature; $t = 0.1$–1.0 ms; energy of the disruption $Q_{dis} = 171$ kJ. The radius of the lithium divertor at strike point was taken as $R = 81.5$ cm [5]. Fig. 3 shows the spatial distribution of the calculated power density along the divertor surface starting from the strike point for two different disruption and ELM durations of 0.1 ms and 0.5 ms. The incident plasma energy is deposited inside the lithium divertor of up to 10 μm in depth (see Fig. 4). The maximum deposition is located at 1 μm below the surface. The net heat load and vaporization rate of the liquid lithium divertor depends on the impact duration, impact energy, and characteristics of the divertor plasma hydrodynamic evolution. The initial plasma impact starts at the strike-point location and initiates vaporization and plasma cloud. Because of plasma shielding effect [21], the impact spot moves along the lithium surface in the x-direction. Fig. 5

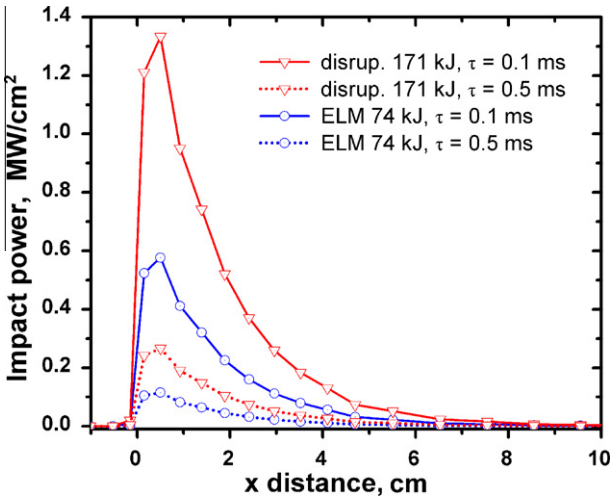

Fig. 3. Calculated initial distributions of impact power along divertor surface during disruptions and ELMs for two different durations.

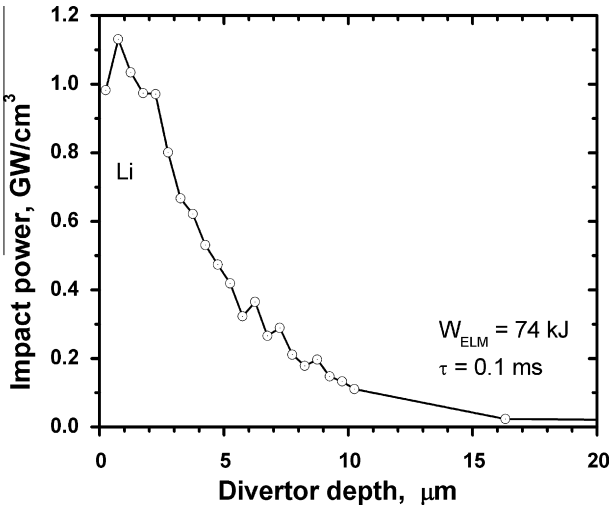

Fig. 4. Depth distribution of deposited plasma power in divertor surface for the 0.1 ms ELM.

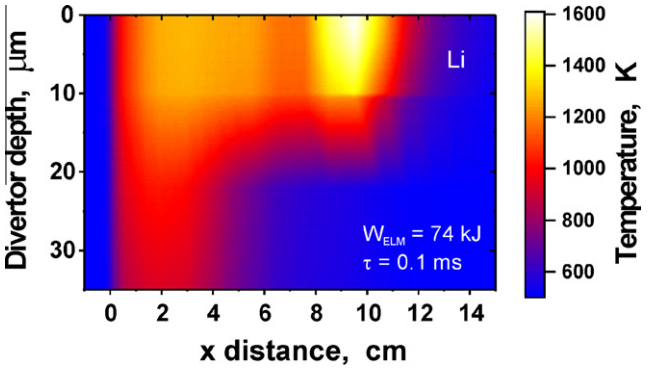

Fig. 5. Temperature distribution along and inside lithium divertor at the end of an ELM of 0.1 ms duration.

shows the temperature distribution in divertor at the end of ELM duration ($t = 0.1$ ms). The hot vaporizing area is shifted here in x-direction from the original spot at the strike point. We should point out the presence of a strong spatial dependence of the divertor heat load and vaporization thickness profile that could not be described with simpler and lower-dimensional models. The complex character of the magnetized plasma drift in the divertor nearby areas did affect the shielding processes of the target lithium plasma. The vaporized lithium cloud starts to heat up and form plasma due to ELM particles continuing impact. The main direction of the initiated lithium plasma is in toroidal direction along the magnetic field lines. Fig. 6 shows two toroidal plasma streams that are moving in opposite directions: the top hot plasma layer moves along y-axis, and the colder closer to divertor surface layer moves in the opposite direction. The toroidal velocities of these streams can achieve values up to 8 km/s. In addition to the toroidal plasma motion, the slow drift in the xz-plane is shown. The toroidal magnetic field is mainly responsible for the convective toroidal motion of the lithium plasma and diffusion across the magnetic field is responsible for vertical and lateral expansion. The diffusive drift velocity has a much less magnitude, only several m/s but can cause material/plasma contamination and expansion to the nearby divertor space, the SOL space, and finally in the bulk core plasma. The final divertor surface vaporization profile (see Fig. 7) is a product of three different time-dependent processes: direct impact energy

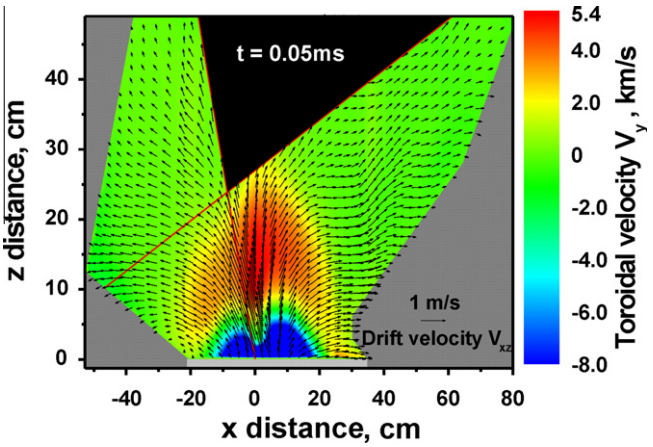

Fig. 6. Velocity distribution of lithium vapor/plasma during an ELM of 0.1 ms duration.

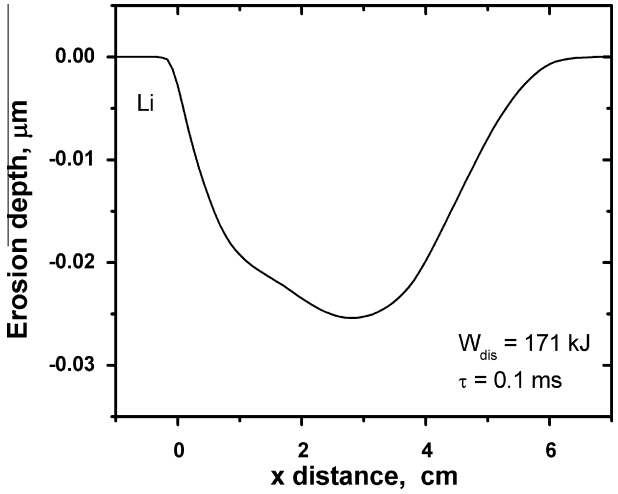

Fig. 7. Lithium surface vaporization thickness during a disruption.

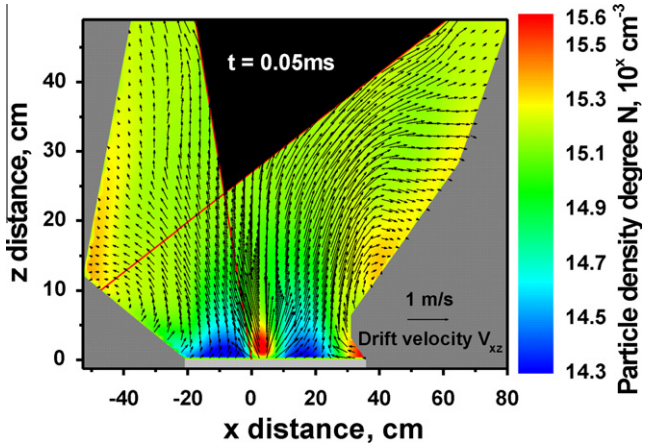

Fig. 8. Lithium expansion above divertor plate and in SOL during an ELM of 0.1 ms duration.

deposition through the unsteady divertor plasma cloud; secondary radiation of the hot plasma cloud; and the thermal conduction of heat inside the divertor plate. Of course this is more of a concern for solid divertor structure than a liquid surface divertor which will not exhibit such profile. The MHD role of the evolved vapor plasma increases considerably with the ELM impact duration. The plasma cloud has sufficient time for motion and expansion in the divertor nearby area. The effectiveness of plasma shielding is reduced and the erosion area concentrates closer to the strike point with deeper erosion on these locations [22]. Again, for a liquid surface this is not so important. Three main locations of the contamination drift can take place: along divertor surface and wall to the SOL, *X*-point area, and at the opposite internal divertor strike point (Fig. 8). The maximum temperature is in the range of 10 eV and is located above the liquid divertor strike point. The motion of the plasma density follows the magnetic field lines from the strike point to *X*-point area and into the SOL space along the device walls. The calculated low radiation fluxes in hundreds of W/cm^2 for the ELM (~10 times higher for disruption) in comparison to the initial particles impact fluxes cannot cause serious damage to nearby components in comparison to ITER ELM and disruption conditions [22]. The radiation fluxes are considerably lower because of the low power of the NSTX device and because of the low-*Z* material of divertor plate.

4. Conclusion

We have developed comprehensive multi-dimensional and multi-fluids models for extensive and integrated simulation of ELMs and disruption plasma impact in NSTX lithium divertor and to assess potential lithium contamination of the plasma near the divertor space. The models include Monte Carlo algorithms for plasma particles motion and collision description; magnetohydrodynamics of the evolving divertor plasma; plasma heat conduction and magnetic field diffusion; weighted Monte Carlo methods for plasma radiation transport; mesh refinement method for the divertor surface detailed energy deposition and surface vaporization models. We studied the ELM and disruption plasma impacts of different durations. The simulation results showed the influence of the 3D MHD geometrical effects on the divertor erosion dynamics. The lithium divertor heat load, divertor surface erosion, and potential lithium contaminations drift were calculated. Lithium expansion in dome and SOL areas can cause bulk plasma contamination during high power ELMs. The secondary radiation fluxes from the shielding plasma cannot cause potential serious damage to nearby components in NSTX in comparison to ITER ELMs and disruption conditions.

Acknowledgement

This work is supplied by the US Department of Energy, Office of Fusion Energy Sciences.

References

[1] M.A. Abdou et al., Fusion Eng. Des. 54 (2001) 181.
[2] S. Mirnov, J. Nucl. Mater. 390–391 (2009) 876.
[3] M.G. Bell et al., Plasma Phys. Control. Fusion 51 (2009) 124054.
[4] J. Sánchez et al., J. Nucl. Mater. 390–391 (2009) 852.
[5] M. Ono et al., Nucl. Fusion 40 (2000) 557.
[6] H.W. Kugel et al., Fusion Eng. Des. 84 (2009) 1125.
[7] R. Maingi et al., J. Nucl. Mater. 337–339 (2005) 727–731.
[8] A. Hassanein, I. Konkashbaev, J. Nucl. Mater. 313–316 (2003) 664.
[9] C. Neumeyer, the NSTX Team, Fusion Eng. Des. 56–57 (2001) 807.
[10] G. Tóth, J. Comput. Phys. 161 (2000) 605.
[11] G. Tóth, D. Odstrčil, J. Comput. Phys. 128 (1996) 82.
[12] G.V. Miloshevsky, V.A. Sizyuk, M.B. Partenskii, A. Hassanein, P.C. Jordan, J. Comput. Phys. 212 (2006) 25.
[13] V. Sizyuk, A. Hassanein, Nucl. Fusion 50 (2010) 115004.
[14] V. Sizyuk, A. Hassanein, Nucl. Fusion 49 (2009) 095003.
[15] V. Sizyuk, A. Hassanein, V. Bakshi, J. Micro/Nanolithography MEMS MOEMS 6 (2007) 043003.
[16] V. Sizyuk, A. Hassanein, T. Sizyuk, Laser Part. Beams 25 (2007) 43.

[17] R.D. Cowan, The Theory of Atomic Structure and Spectra, Univ. of California Press, Berkley, 1981.
[18] V. Tolkach, V. Morozov, A. Hassanein, Development of Comprehensive Models for Opacities and Radiation Transport for IFE Systems, Argonne National Laboratory Report ANL-ET/02-23, Argonne, IL, 2002.
[19] H. Yong, J. Zhonghe, X. Shengguo, Plasma Sci. Technol. 5 (2003) 1795.
[20] I. Konkashbaev, A. Hassanein, R. Maingi, NSTX: SOL and Divertor Plate During ELMs, Plasma Facing Components Community Meeting, Livermore, CA, December 5–7, 2004.
[21] H. Würz et al., J. Nucl. Mater. 233–237 (1996) 798.
[22] A. Hassanein, T. Sizyuk, V. Sizyuk, G. Miloshevsky, Fusion Eng. Des. 85 (2010) 1331.